Influence of Lanthanum on the Surface Structure and CO Hydrogenation Activity of Supported Cobalt Catalysts

Jeffrey S. Ledford, Marwan Houalla, Andrew Proctor, David M. Hercules,*

Department of Chemistry, University of Pittsburgh, Pittsburgh, Pennsylvania 15260

and Leonidas Petrakis†

Gulf Research & Development, P.O. Box 2038, Pittsburgh, Pennsylvania 15230 *(Received: January 17, 1989)*

X-ray photoelectron spectroscopy (ESCA or XPS), X-ray diffraction (XRD), Raman spectroscopy, H_2 chemisorption, and gravimetric analysis have been used to characterize three series of La/Al_3O_3 and $CoLa/Al_2O_3$ catalysts. $CoLa/Al_2O_3$ catalysts were prepared by two methods: impregnation of La first followed by Co (designated "CoLa*y*") and impregnation of Co first followed by La (designated "La*y*Co"). The information obtained from surface and bulk characterization has been compared with CO hydrogenation activity and selectivity of the supported Co/Al_2O_3 catalysts. For CoLa*y* catalysts with low La loadings (La/Al atomic ratio ≤ 0.026), the presence of La had little effect on the structure or CO hydrogenation activity. However, the selectivity to higher hydrocarbons and olefinic products increased with increasing La content. For CoLa*y* catalysts with higher La loadings, Co_3O_4 is suppressed in favor of an amorphous dispersed La–Co mixed oxide. ESCA and H_2 chemisorption indicated higher dispersion of the metallic cobalt phase for high La loadings. The turnover frequency (TOF) for CO hydrogenation decreased dramatically for high La loadings. This has been correlated to the decrease in the amount of Co_3O_4 present in the La-rich catalysts. Catalysts prepared by reverse impregnation (La*y*Co) showed little evidence of La–Co interaction. No significant variation in reducibility or cobalt metal dispersion was observed. Lanthanum addition had little effect on the TOF for CO hydrogenation or the selectivity to olefinic products and higher hydrocarbons.

Introduction

Industrial cobalt Fisher–Tropsch catalysts are normally multicomponent systems consisting of one or more promoters in addition to the supported metal. Rare earth oxides are often used as promotors in Ni-, Co-, and Fe-based CO hydrogenation catalysts.[1-11] The promotion effect of these additives is generally attributed to two processes: (a) coverage of the surface of the active phase by the promoter resulting in a decrease in chemisorption capacity and the creation of new catalytic sites at the metal–promoter interface[1] and/or (b) the presence of partially reduced promoter oxides which provide binding sites for the oxygen end of the CO molecule facilitating dissociation of the C–O bond.[2,3] Recently, Barrault et al.[1] reported that lanthanum or cerium promotion of a carbon-supported cobalt catalyst improves the activity and increases the selectivity to olefins and higher hydrocarbons. This promotion effect was attributed to the formation of new active sites by the migration of patches of partially reduced rare earth oxides to the surface of cobalt during activation.

Previous studies of rare earth promoters[1-11] have focused primarily on their effects on catalyst activity and selectivity. Little effort has been devoted to investigating systematically the effect of these promoters on the structure and reactivity of the active phase. The present work is part of a broad study to investigate the effects of rare earth and actinide promoters on the structure and reactivity of group VIII metal based CO hydrogenation catalysts. X-ray photoelectron spectroscopy (XPS, ESCA), X-ray diffraction (XRD), Raman spectroscopy, gravimetric analysis, and H_2 chemisorption were used to examine the influence of lanthanum on the state and dispersion of cobalt supported on alumina. The information derived from these techniques is correlated with the CO hydrogenation activity and selectivity of supported cobalt catalysts.

Experimental Section

Catalyst Preparation. The La-modified alumina carriers (La/Al_2O_3) were prepared by pore volume impregnation of γ-alumina (Harshaw 1401, nominal surface area 180 m^2/g) with solutions of lanthanum nitrate (Fisher Purified). The samples were dried at 110 °C for 12 h and calcined at 400 °C for 8 h. The lanthanum content of the La/Al_2O_3 series was varied from an La/Al atomic ratio of 0 to 0.078 (0 to 25 wt % La_2O_3).

$CoLa/Al_2O_3$ catalysts were prepared by pore volume impregnation of the La-modified alumina carriers using solutions of cobalt nitrate (Fisher Certified ACS). Drying and calcination conditions were the same as those used for the La/Al_2O_3 series. The cobalt content of the samples was held constant at 10 wt % of the alumina support. $Co/La/Al_2O_3$ samples will be designated by "CoLa*y*", where *y* is the La/Al atomic ratio ($\times 10^2$). Several cobalt–lanthanum catalysts were prepared by reverse impregnation of Co/Al_2O_3 catalysts using solutions of lanthanum nitrate (designated "La*y*Co"). Drying and calcination conditions were the same as those used for the "CoLa*y*" preparations. It should be noted that the Co/Al_2O_3 catalyst used to prepare the La*y*Co series is a different preparation from the Co/Al_2O_3 catalyst used in the CoLa*y* series.

Standard Materials. Co_3O_4 (99.5%) was obtained from Cerac Inc., $La(OH)_3$ (99.9%) and $CoAl_2O_4$ (98%) were obtained from Alfa Products, and $La_2(CO_3)_3$ (99.9%) was obtained from Pfaltz & Bauer. La_2O_3 was prepared by heating lanthanum nitrate (Fisher Purified) in air at 800 °C for 8 h. $LaCoO_3$ was prepared by calcination of an amorphous precursor at 600 °C for 4 h. The $LaCoO_3$ precursor was a slurry obtained by concentrating an aqueous solution of metal nitrates and citric acid. $LaAlO_3$ was prepared by calcining stoichiometric amounts of the respective nitrates (Fisher Certified ACS) in air at 1100 °C for 8 h. XRD patterns of all the standard compounds matched the appropriate ASTM powder diffraction file.

† Present address: Chevron Research Company, P.O. Box 1627, Richmond, CA 94802.

(1) Barrault, J.; Guilleminot, A.; Achard, J. C.; Paul-Boncour, V.; Percheron-Guegan, A. *Appl. Catal.* **1986**, *21*, 307–312.
(2) Fleisch, T. H.; Hicks, R. F.; Bell, A. T. *J. Catal.* **1984**, *87*, 398–413.
(3) Rieck, J. S.; Bell, A. T. *J. Catal.* **1985**, *96*, 88–105.
(4) Sauvion, G. N.; Tempere, J. F.; Guilleux, M. F.; Mariadassou, G. D.; Delafosse, D. *J. Chem. Soc., Faraday Trans. 1* **1985**, *81*, 1357–1367.
(5) Gelsthorpe, M. R.; Mok, K. B.; Ross, J. R. H.; Sambrook, R. M. *J. Mol. Catal.* **1984**, *25*, 253–262.
(6) Inui, T.; Ueno, K.; Funabiki, M.; Suehiro, M.; Sezume, T.; Takegami, Y. *J. Chem. Soc., Faraday Trans. 1* **1979**, *75*, 787–802.
(7) Kieffer, R.; Kiennemann, A.; Rodriguez, M.; Bernal, S.; Rodriguez-Izquierdo, J. M. *Appl. Catal.* **1988**, *42*, 77–89.
(8) Schaper, H.; Doesburg, E. B. M.; De Korte, P. H. M.; Van Reijen, L. L. *Appl. Catal.* **1985**, *14*, 371–379.
(9) Xie, Y. C.; Qian, M. X.; Tang, Y. Q. Presented at the China–Japan–U.S. Symposium of Heterogeneous Catalysis Related to Energy Problems, B.10C Dalian, China, 1982.
(10) Chen, Y. W.; Goodwin, J. G., Jr. *React. Kinet. Catal. Lett.* **1984**, *26*(3–4), 453–459.
(11) Baker, B. G.; Clark, N. J. *Stud. Surf. Sci. Catal.* **1987**, *31*, 455–465.

0022-3654/89/2093-6770$01.50/0

X-ray Diffraction. X-ray powder diffraction patterns were obtained with a Diano XRD-6 diffractometer employing Ni-filtered Cu Kα radiation (1.54056 Å). The X-ray tube was operated at 50 kV and 25 mA. Catalysts were run as pellets on a glass slide. Spectra were scanned at a rate of 0.2 deg/min (in 2θ).

Quantitative X-ray diffraction data were obtained from absolute intensities of the Co_3O_4 ⟨511⟩ peak (59.4° in 2θ). We have found that, for Co/Al_2O_3 catalysts impregnated with $La(NO_3)_3$ solutions (dried La*y*Co), Co_3O_4 XRD intensities decrease with increasing lanthanum loading. For the dried La7.8Co catalyst, the Co_3O_4 intensity was 50% of the value measured for unpromoted Co/Al_2O_3. Since it is unlikely that addition of $La(NO_3)_3$ to a Co/Al_2O_3 catalyst will disrupt the structure of crystalline Co_3O_4, a possible explanation for the decrease in Co_3O_4 intensity is that part of the Cu Kα radiation diffracted from Co_3O_4 particles is absorbed by lanthanum. Indeed, lanthanum is well-known as a heavy absorber in X-ray fluorescence.[12] X-ray fluorescence results indicate that nitric acid solution (pH = 2) can be used to extract lanthanum to a level corresponding to La/Al atomic ratio of approximately 0.0075. Following removal of lanthanum from the dried La7.8Co catalyst, the Co_3O_4 XRD intensity was identical with the value observed for the unpromoted catalyst. We found that extraction of lanthanum from calcined CoLa*y* and La*y*Co catalyst with La/Al atomic ratios >0.013 increases the Co_3O_4 XRD intensity; Co_3O_4 intensities are thus reported for extracted CoLa*y* and La*y*Co catalysts. Co_3O_4 ⟨511⟩ peak areas were measured with an Apple II plus computer assuming a linear background over the peak base. Ratios of peaks from the supported phase and the alumina carrier were not used for quantification because of the possibility that cobalt and/or lanthanum addition disrupts the Al_2O_3 spinel and subsequently affects the intensity of the alumina peaks. All quantitative measurements for a series of catalysts were completed in 4 h to minimize the effects of X-ray source and detector fluctuations. The error in this method was estimated to be ±20%.

The mean crystallite size of the Co_3O_4 phase ($\bar{d}$) was determined from XRD line broadening measurements using the Scherrer equation:[13]

$$\bar{d} = K\lambda/\beta \cos\theta \qquad (1)$$

where λ is the X-ray wavelength, K is the particle shape factor, taken as 0.9, and β is the full width at half-maximum (fwhm), in radians, of the Co_3O_4 ⟨511⟩ line. Reported crystallite sizes were corrected for instrumental broadening as described by Klug and Alexander.[13]

Raman Spectra. Raman spectra were recorded on a Spex Ramalog spectrometer equipped with holographic gratings. The 5145-Å line from a Spectra-Physics Model 165 argon ion laser was used as the exciting source. The spectral slit width was 4 cm^{-1}; a laser power of 50 mW measured at the sample was used. The samples were pressed into pellets with KBr as a support. Excessive heating of the sample was minimized by rotating the pellet off axis so that irradiation of a given area of the sample was not continuous. Peak areas of the 693-cm^{-1} Raman line of Co_3O_4 were integrated by use of a Spex Datamate computer assuming a linear background over the peak width. All quantitative measurements for a series of catalysts were completed in 8 h to minimize the effects of laser power and detector fluctuations. The error in this method is estimated to be ±15%.

ESCA Spectra. ESCA spectra of oxidic catalysts were obtained by means of a Leybold-Heraeus LHS-10 electron spectrometer equipped with an aluminum anode (1486.6 eV) operated at 240 W (12 kV, 20 mA). The spectrometer was interfaced to an HP1000 minicomputer. The instrument typically operates at pressures below 1×10^{-8} Torr in the analysis chamber. ESCA spectra of oxidic catalysts were also obtained with a Hewlett-Packard 5950A electron spectrometer equipped with a monochromatized aluminum anode (1486.6 eV) operated at 600 W. The spectrometer was interfaced to an IBM PC. The instrument typically operates at pressures below 1×10^{-9} Torr in the analysis chamber. ESCA measurements of reduced CoLa*y* catalysts were performed with an AEI-ES200A spectrometer using an Al anode operated at 264 W (12 kV, 22 mA). The spectrometer was interfaced to an Apple II plus computer. The AEI-ES200A instrument typically operates at pressures below 1×10^{-8} Torr in the analysis chamber. ESCA analysis of reduced CoLa*y* catalysts was performed using a sealable probe which allowed transfer of samples from a tube reactor to the AEI-ES200A spectrometer without exposure to air.[14] ESCA analysis of reduced La*y*Co catalysts was performed using a reactor attached to the LHS-10 spectrometer.[15] In each case, reduction was carried out by flowing H_2 (100 cm^3/min, 99.999%) over the catalysts for 12 h. The Al 2p line from the support was used as the binding energy reference (74.5 eV). The binding energies for standard compounds that did not contain Al were referenced to the C 1s line (284.6 eV) of the carbon overlayer. The binding energies for $CoAl_2O_4$ and $LaAlO_3$ were referenced to the Al 2p line (74.5 eV). ESCA binding energies were measured with a precision of ±0.2 eV, or better.

Quantitative ESCA Analysis. It has been shown by Defosse et al.[16] that one may calculate the theoretical intensity ratio ($I_m°/I_s°$) expected for a supported phase (m) atomically dispersed on a carrier (s). An extension of the Defosse model proposed by Kerkhof and Moulijn[17] has been used in the present investigation. The photoelectron cross sections and the mean escape depths of the photoelectrons used in these calculations are taken from Scofield[18] and Penn,[19] respectively.

For a phase (m) present as discrete particles, the experimental intensity ratio (I_m/I_s) is given by the following expression:

$$I_m/I_s = (I_m°/I_s°)[1 - \exp(-d/\lambda_m)]/(d/\lambda_m) \qquad (2)$$

where d is the length of the edge of the cubic crystallites of the deposited phase and λ_m is the mean escape depth of the photoelectrons in m. The cobalt metal dispersion determined from ESCA is calculated assuming that five sides of the cubic particle are exposed and a site density of 14.6 atoms/nm^2.[20]

It must be stressed however that the validity of the Kerkhof–Moulijn model depends on a homogeneous distribution of the supported phase over the carrier.[17,21] It is also assumed that addition of the supported phase does not affect the surface area of the carrier.[17]

Gravimetric Analysis. Gravimetric analysis was carried out using a Cahn 113 microbalance. Approximately 100 mg of catalyst was dried for 4 h at 435 °C in a flow of 10% O_2/He (99.999%) prior to reduction. Reduction was carried out at 400 °C for 12 h in a flow of H_2 (99.999%). Samples were reoxidized for 4 h at 435 °C in a flow of 10% O_2/He (99.999%). The extent of cobalt reduction was calculated from the weight change which occurred on reoxidation.

Hydrogen Chemisorption. Hydrogen chemisorption was performed in a conventional stainless steel volumetric system evacuated by mechanical and oil diffusion pumps. The base pressure of the system was approximately 5×10^{-6} Torr. An MKS-390 Baratron Pressure Transducer was used for pressure measurements over a range of 0–1000 Torr. Following reduction in H_2 (99.999%) for 12 h at 400 °C, the samples were evacuated for 1 h at 300

(12) Norrish, K.; Chappell, B. W. X-ray Fluorescence Spectrometry. In *Physical Methods in Determinative Mineralogy*; Zussman, J., Ed.; Academic Press: London, 1977; pp 201–272.
(13) Klug, H. P.; Alexander, L. E. *X-ray Diffraction Procedures for Polycrystalline and Amorphous Materials*, 1st ed.; Wiley: New York, 1954.
(14) Patterson, T. A.; Carver, J. C.; Leyden, D. E.; Hercules, D. M. *J. Phys. Chem.* **1976**, *80*, 1700–1708.
(15) Ledford, J. S.; Hoffmann, D. P.; Proctor, A.; Hercules, D. M. To be submitted for publication.
(16) Defosse, C.; Canesson, D.; Rouxhet, P. G.; Delmon, B. *J. Catal.* **1978**, *51*, 269–277.
(17) Kerkhof, F. P. J. M.; Moulijn, J. A. *J. Phys. Chem.* **1979**, *83*, 1612–1619.
(18) Scofield, J. H. *J. Electron Spectrosc. Relat. Phenom.* **1976**, *8*, 129–137.
(19) Penn, D. R. *J. Electron Spectrosc. Relat. Phenom.* **1976**, *9*, 29–40.
(20) Young, R. S. *Cobalt, Its Chemistry, Metallurgy and Uses*; Reinhold: New York, 1948.
(21) Delannay, F.; Houalla, M.; Pirotte, D.; Delmon, B. *Surf. Interface Anal.* **1979**, *1*, 172–174.

TABLE I: Effect of Lanthanum and Cobalt Content on the BET Surface Areas of La*y*, CoLa*y*, and La*y*Co Catalysts

La/Al atomic ratio (×10²)	BET surface area, m²/g		
	La*y*	CoLa*y*	La*y*Co
0.0	180	171	171
0.3	209	183	*a*
0.5	204	176	*a*
1.3	200	183	158
2.6	182	169	144
4.3	157	144	144
6.1	147	145	119
7.8	135	139	109

[a] Catalysts were not prepared.

°C. Following evacuation, the samples were cooled to 25 °C to perform the adsorption experiment. Adsorption isotherms were measured by the adsorption (increasing pressure) method after the evacuation period. The H_2 uptake was calculated by extrapolating the linear portion of the adsorption isotherm to 0 Torr. The number of exposed Co atoms was determined from the total H_2 uptake. Cobalt metal dispersion is defined as the ratio of the number of exposed cobalt atoms to the total number of metal atoms determined from gravimetric analysis.

CO Hydrogenation Activity. Measurement of CO hydrogenation activity was performed in a flow microreactor with a 25 cm³/min flow of H_2/CO/He (9%/3%/88%) at 185 °C. Reactant gas flow rates were held constant with Matheson mass flow controllers, and reactor temperatures were fixed by use of Honeywell DC100 controllers. Product gases were passed through a heated transfer line to a Perkin-Elmer Sigma 2000 gas chromatograph. Hydrocarbons were separated on a 6-m packed column containing Chromosorb 102. Olefin/paraffin separation was achieved by means of a 6-m packed column containing VZ-10. The chromatograph was interfaced to a Perkin-Elmer LCI-100 integrator for data analysis. Activity measurements were performed at conversions less than 5%. Selectivities are reported for catalysts operated at similar conversions.

Results

Lanthanum-Modified Aluminas. Results for the lanthanum-modified aluminas (La*y*) have been reported elsewhere[22] but are summarized here to highlight the effect of cobalt addition to the La-modified carriers.

Variation of the BET surface areas of the modified aluminas (La*y*) as a function of the lanthanum content is given in Table I. There is an initial 15% increase in the surface area with La addition followed by a steady decrease as the carrier is enriched in lanthanum. XRD patterns of the La-modified aluminas showed only lines characteristic of the alumina carrier. The ESCA La $3d_{5/2}$ binding energies measured for the La*y* series (836.1 ± 0.2 eV) were independent of La content and higher than the values measured for $LaAlO_3$ (835.7 eV), $La_2(CO_3)_3$ (835.5 eV), $La(OH)_3$ (834.8 eV), or La_2O_3 (833.5 eV).

Variation of the (La $3d_{5/2}$)/(Al 2p) intensity ratio as a function of the La/Al atomic ratio is shown for the La*y* catalysts (full circles) in Figure 1. The theoretical line calculated for monolayer dispersion of lanthanum is shown for comparison. The La/Al intensity ratios measured for the La*y* catalysts are approximately 80% of the value calculated for monolayer dispersion. However, for catalysts with La/Al > 0.026, the values calculated for monolayer dispersion must be considered as lower estimates because of the observed decrease in catalyst surface area (Table I).

Cobalt/Lanthanum/Alumina Catalysts (Lanthanum First). The BET surface areas of the CoLa*y* catalysts were generally lower than those of the modified aluminas (Table I). The XRD pattern of the CoLa0 catalyst showed diffraction lines characteristic of Co_3O_4 (Figure 2a). The ⟨511⟩ XRD line of Co_3O_4 is readily observed in the diffraction patterns of extracted CoLa*y* catalysts with La/Al atomic ratios ≤0.043 (Figure 2a). However,

(22) Ledford, J. S.; Houalla, M.; Petrakis, L.; Hercules, D. M. *Stud. Surf. Sci. Catal.* **1987**, *31*, 433–442.

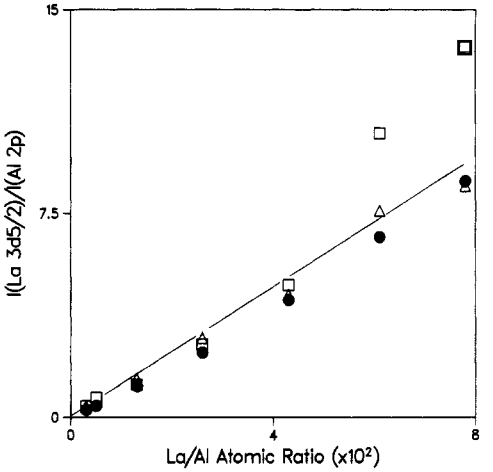

Figure 1. ESCA (La $3d_{5/2}$)/(Al 2p) intensity ratios of La*y* (●), CoLa*y* (□), and La*y*Co (△) catalysts plotted versus La/Al atomic ratio. (La $3d_{5/2}$)/Al 2p) intensity ratios calculated for monolayer dispersion (line).

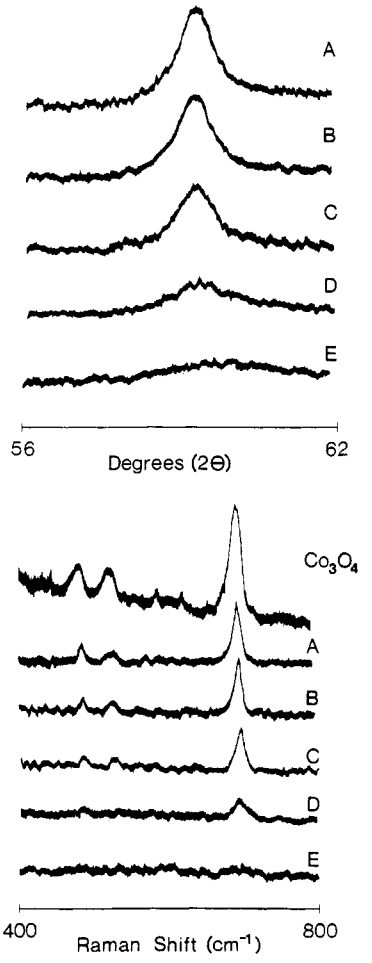

Figure 2. (a, top) X-ray diffraction patterns of the Co_3O_4 ⟨511⟩ line measured for extracted CoLa*y* catalysts. (b, bottom) Raman spectra measured for Co_3O_4 and selected CoLa*y* catalysts. (A) CoLa0, (B) CoLa2.6, (C) CoLa4.3, (D) CoLa6.1, (E) CoLa7.8.

for higher La contents, the Co_3O_4 peaks were sharply reduced. Variation of the intensity measured for the ⟨511⟩ XRD line of Co_3O_4 is given as a function of La/Al atomic ratio in Figure 3 (closed circles). The intensities have been normalized to the value measured for the unpromoted Co/Al_2O_3 catalyst. For CoLa*y* catalysts with La/Al ≤0.026, the intensities are identical, within experimental error, with the value measured for the unpromoted catalyst. For the CoLa6.1 catalyst, the intensity of the Co_3O_4 peak decreases to approximately 30% of the value measured for the unpromoted catalyst. No ⟨511⟩ Co_3O_4 peak can be observed

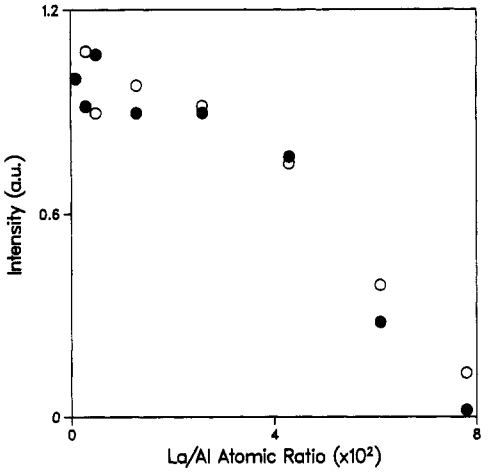

Figure 3. Intensities of the XRD (●) and Raman (○) peaks for Co_3O_4 obtained from CoLay catalysts plotted versus La/Al atomic ratio.

for the CoLa7.8 catalyst. X-ray diffraction line broadening calculations indicated that, for CoLay catalysts with La/Al atomic ratios up to 0.043, the Co_3O_4 crystallite size was approximately 11.8 ± 1.0 nm. The Co_3O_4 particle size calculated for the CoLa6.1 catalyst was approximately 7.0 nm.

Raman spectra of CoLay catalysts (Figure 2b) showed peaks characteristic of Co_3O_4 (485, 524, and 693 cm^{-1}).[23] The intensities of the Co_3O_4 lines were independent of lanthanum loading up to a La/Al atomic ratio of 0.026. For higher La loadings, the Co_3O_4 intensity decreased with increasing La content. Variation of the intensity measured for the 693-cm^{-1} Raman line of Co_3O_4 is given as a function of La/Al atomic ratio in Figure 3 (open circles). The intensities have been normalized to the value measured for the unpromoted Co/Al_2O_3 catalyst. The intensity reported for the CoLa7.8 catalyst is the average of eight scans summed to improve the signal/noise of the spectrum. For catalysts with La/Al ≤0.026, increasing the lanthanum content of the La/Al_2O_3 has little effect on the intensity of the Raman line for Co_3O_4. For catalysts with La/Al >0.026, the Co_3O_4 Raman intensity decreases with increasing lanthanum loading. For CoLa6.1 and CoLa7.8 catalysts, the intensities of the Co_3O_4 peaks were 40% and 15%, respectively, of the value measured for the unpromoted catalyst.

The La $3d_{5/2}$ binding energies measured for the CoLay catalysts (836.1 ± 0.2 eV) are identical with the values measured for the Lay catalysts and do not vary with La loading. Comparison of the (La $3d_{5/2}$)/(Al 2p) intensity ratios measured for the CoLay catalysts and the Lay carriers indicates that addition of cobalt to the Lay carriers increases the La/Al ESCA intensity ratios (Figure 1).

The Co $2p_{3/2}$ spectra of several CoLay catalysts are shown in Figure 4. The addition of lanthanum had little effect on the Co $2p_{3/2}$ binding energies measured for the catalysts (781.5 ± 0.2 eV). The Co $2p_{3/2}$ binding energies measured for the catalysts are lower than the value measured for $CoAl_2O_4$ (781.9 eV) and higher than values obtained for Co_3O_4 (780.3 eV) and $LaCoO_3$ (779.9 eV). For low loadings of La (La/Al ≤0.026), the intensity of the shake-up satellite (~787.5 eV) decreases with increasing La loading. For catalysts with higher La loadings (La/Al ≥0.026), the shake-up satellite at ~787.5 eV cannot be readily detected.

Variation of the ESCA (Co $2p_{3/2}$)/(Al 2p) intensity ratios measured for CoLay catalysts is shown as a function of La content in Figure 5. The theoretical line calculated for monolayer dispersion of cobalt is also shown for comparison. As noted in the case of Lay catalysts, the monolayer model does not strictly apply for La-rich catalysts. Intensity ratios measured for catalysts obtained from cobalt impregnation of the Lay carriers but before calcination (dried) are slightly higher than the predicted monolayer value and do not vary significantly with La loading (open circles).

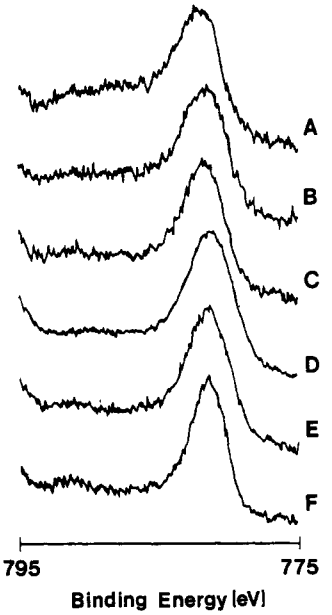

Figure 4. ESCA Co $2p_{3/2}$ spectra measured for oxidic CoLay catalysts: (A) CoLa0, (B) CoLa1.3, (C) CoLa2.6, (D) CoLa4.3, (E) CoLa6.1, and (F) CoLa7.8.

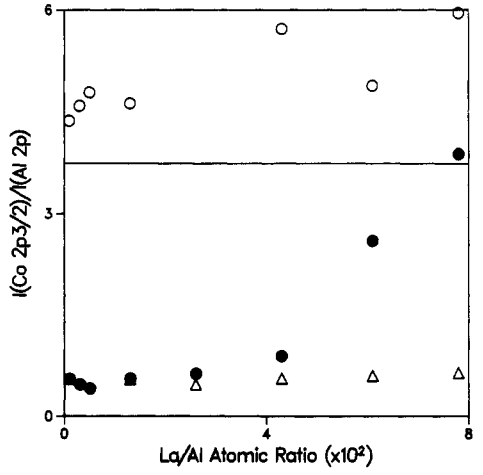

Figure 5. ESCA (Co $2p_{3/2}$)/(Al 2p) intensity ratios of dried CoLay catalysts (○), calcined CoLay catalysts (●), and calcined LayCo catalysts (△) plotted versus La/Al atomic ratio. (Co $2p_{3/2}$)/(Al 2p) intensity ratios for monolayer dispersion (line).

Variation of the (Co $2p_{3/2}$)/(Al 2p) intensity ratio measured for the calcined CoLay catalysts (closed circles) as a function of La/Al atomic ratio is also shown in Figure 5. For oxidic catalysts with La/Al atomic ratios ≤0.026, the measured intensity ratios are approximately 15% of the value calculated for monolayer dispersion (3.75). A drastic increase in the measured intensity ratio is observed as the La content of the catalysts increases.

The Co $2p_{3/2}$ spectra measured for the reduced CoLay catalysts showed peaks at 781.2 ± 0.2 and 778.1 ± 0.2 eV, characteristic of unreduced cobalt surface phase and metallic cobalt, respectively.[24] The La $3d_{5/2}$ binding energy measured for reduced CoLay catalysts decreased from 836.0 to 835.3 eV with increasing La loading. The reducibility of cobalt as a function of the La/Al atomic ratio of the CoLay catalysts determined from both ESCA and gravimetric measurements is given for several catalysts in Table II. For catalysts with La/Al atomic ratios ≤0.026, the ESCA and gravimetric data indicate that addition of La does not significantly affect the reducibility of the cobalt phase. A decrease in the extent of reduction from approximately 85% to 50% is observed with a further increase in La loading.

(23) Hadjev, V. G.; Iliev, M. N.; Vergilov, I. V. *J. Phys. C* **1988**, *21*, L199–L204.

(24) Stranick, M. A.; Houalla, M.; Hercules, D. M. *J. Catal.* **1987**, *103*, 151–159.

TABLE II: Reducibility and Dispersion of CoLa*y* Catalysts[a]

La/Al atomic ratio (×10²)	reducibility		dispersion	
	ESCA	gravimetric	ESCA	chemisorption
0.0	89	84	10.5	4.4
0.3	88	87	11.7	4.1
0.5	85	80	12.3	4.8
1.3	95	87	10.3	5.2
2.6	83	87	14.7	6.5
4.3	73	85	16.3	6.7
6.1	(64)[b]	72	(46.4)[b]	6.7
7.8	(49)[b]	51	(100)[b]	10.7

[a] Relative standard deviations for data are ±10%. [b] Values for these catalysts must be considered as approximates due to uncertainty in calculations (see text).

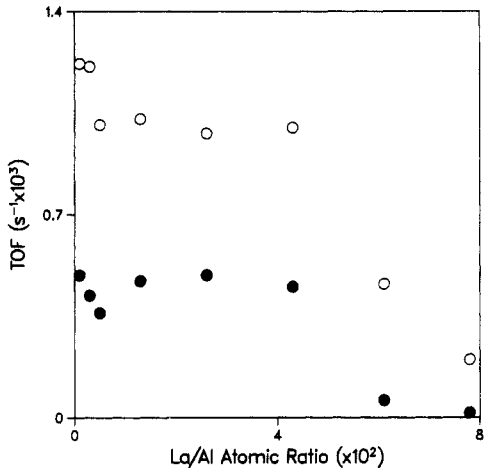

Figure 6. Variation of the turnover frequency (TOF) for CO hydrogenation measured for CoLa*y* catalysts using H_2 chemisorption (○) and ESCA estimates (●) of Co metal dispersion.

Table II shows the variation of cobalt metal dispersion as a function of La content calculated from H_2 chemisorption and ESCA data. For catalysts with La/Al atomic ratios <0.026, addition of lanthanum had little effect on the cobalt metal dispersion calculated for ESCA. For higher La loadings, the cobalt metal dispersion increases dramatically with increasing La content. Cobalt metal dispersions calculated from chemisorption data were significantly lower than the values estimated from ESCA results. ESCA data show a much greater increase in cobalt dispersion for the CoLa6.1 and CoLa7.8 catalysts, compared to H_2 chemisorption.

Variation of the TOF for CO hydrogenation based on H_2 chemisorption (open circles) and ESCA estimates (closed circles) of Co metal dispersion is given as a function of La/Al atomic ratio of the CoLa*y* catalysts in Figure 6. For catalysts with La/Al ratios <0.043, La addition has little effect on the TOF calculated by using ESCA and H_2 chemisorption estimates of Co metal dispersion. A significant decrease in TOF is observed for La-rich catalysts. Turnover frequencies calculated from H_2 chemisorption data show a less pronounced decrease relative to those determined from ESCA data.

Table III shows the influence of La content on the weight fraction of (C2+) products and the olefin/paraffin selectivity measured for the CoLa*y* catalysts. The fraction of C2+ produced by the catalysts increases from approximately 65 to 80 wt % as the La content increases. For catalysts with La/Al atomic ratios <0.013, lanthanum addition has little effect on the olefin/paraffin ratio (C2–C4) produced by the catalysts. However, for catalysts with higher La contents, the olefin/paraffin ratio increases up to a factor of 2 with increasing La content.

Lanthanum/Cobalt/Aluminum Catalysts (Lanthanum Second). The BET surface areas of the La*y*Co catalysts were lower than those measured for the CoLa*y* catalysts (Table I). XRD patterns for catalysts prepared by reverse impregnation (La*y*Co) all showed diffraction lines characteristic of Co_3O_4. The intensity

TABLE III: Influence of Lanthanum Content on Selectivity of CoLa*y* and La*y*Co Catalysts to Higher Hydrocarbons and Olefins (wt %)

La/Al atomic ratio (×10²)	CoLa*y* catalysts		La*y*Co catalysts	
	C2+	O/P	C2+	O/P
0.0	65	4.8	65	4.8
0.3	66	5.0	*a*	*a*
0.5	68	5.1	*a*	*a*
1.3	68	6.6	64	4.8
2.6	74	7.6	65	4.8
4.3	79	7.5	63	4.8
6.1	79	11.0	63	5.1
7.8	81	10.3	64	4.4

[a] Catalysts were not prepared.

TABLE IV: Reducibility and Dispersion of La*y*Co Catalysts[a]

La/Al atomic ratio (×10²)	reducibility		dispersion	
	ESCA	gravimetric	ESCA	chemisorption
0	90	84	14.8	4.7
1.3	92	*c*	13.1	4.6
2.6	92	87	11.2	5.5
4.3	*b*	*c*	*b*	4.8
6.1	*b*	*c*	*b*	5.6
7.8	*b*	80	*b*	4.8

[a] Relative standard deviations for data are ±10%. [b] Values cannot be calculated due to La Kβ interference with Co 2p peaks (see text). [c] Gravimetric analysis was not performed for these catalysts.

of the Co_3O_4 ⟨511⟩ line does not vary significantly with La content. XRD line broadening calculations indicated that the Co_3O_4 crystallite size was approximately 12.5 ± 1.0 nm for all La*y*Co catalysts.

Raman spectra of La*y*Co catalysts showed peaks characteristic of Co_3O_4. As observed by XRD, La addition has little effect on the intensity of the Co_3O_4 peaks measured by Raman spectroscopy.

The La $3d_{5/2}$ binding energies measured for the La*y*Co catalysts (836.2 ± 0.2 eV) are identical, within experimental error, with the values measured for CoLa*y* catalysts. The (La $3d_{5/2}$)/(Al 2p) intensity ratios measured for the La*y*Co catalysts (open triangles, Figure 1) are identical, within experimental error, with the values measured for the La*y* catalysts.

The Co $2p_{3/2}$ binding energies measured for the La*y*Co catalysts (781.6 ± 0.2 eV) are identical, within experimental error, with the values measured for CoLa*y* catalysts. The background beneath the Co 2p peak increases with increasing La loading due to the presence of the La $M_{45}N_{45}V$ Auger line. Thus, we cannot accurately determine the effect of La addition on the Co 2p peak shape. Lanthanum addition has little effect on the (Co $2p_{3/2}$)/(Al 2p) intensity ratios measured for the oxidic La*y*Co catalysts (open triangles, Figure 5).

The Co $2p_{3/2}$ spectra measured for reduced La*y*Co catalysts had peaks at 781.5 ± 0.3 and 777.8 ± 0.2 eV, corresponding to unreduced surface phase and cobalt metal, respectively.[24] Table IV shows the variation of cobalt reducibility and cobalt metal dispersion calculated for the La*y*Co catalysts as a function of La/Al atomic ratio. The reducibility of the La0Co catalyst is identical, within experimental error, with the value obtained for the CoLa0 catalyst. However, the cobalt metal dispersion calculated for the La0Co catalyst by using ESCA data is slightly higher than the value measured for the CoLa0 catalyst. For La*y*Co catalysts with La/Al atomic ratios <0.026, La addition has little effect on the cobalt reducibility and cobalt metal dispersion. For catalysts, with higher La loadings, interference from La Kβ X-ray satellite lines makes accurate calculation of Co 2p intensities impossible. Thus, we cannot calculate the extent of cobalt reduction or the cobalt metal dispersion for La-rich La*y*Co catalysts.

Variation of the TOF for CO hydrogenation based on H_2 chemisorption (open circles) and ESCA estimates (closed circles) of Co metal dispersion is given as a function of La/Al atomic ratio of the La*y*Co catalysts in Figure 7. For La-rich catalysts (La/Al

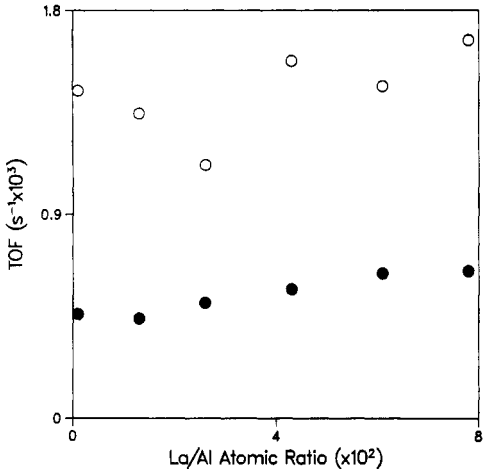

Figure 7. Variation of the turnover frequency (TOF) for CO hydrogenation measured for LayCo catalysts using H_2 chemisorption (O) and ESCA estimates (●) of Co metal dispersion.

≥0.043), turnover frequencies calculated by using ESCA estimates of Co metal dispersion are based on an average dispersion determined from catalysts with lower La loadings. This approximation is supported by the absence of any significant change in Co metal dispersion determined by H_2 chemisorption data. In contrast to the case for CoLay catalysts where a sharp decrease in TOF was observed for high La loadings, the TOF measured for LayCo catalysts increases slightly with increasing La loading.

Variation of the weight fraction of higher hydrocarbons (C2+) and olefin/paraffin ratio (C2–C4) produced by the LayCo catalysts as a function of La/Al atomic ratio is given in Table III. The addition of La has little effect on the selectivity to higher hydrocarbons and olefinic products.

Discussion

Structure of Lanthanum/Alumina Catalysts. The absence of XRD peaks characteristic of discrete La phases and the similarity of the La/Al intensity ratios measured for the catalysts with the values calculated for monolayer dispersion suggest that lanthanum is highly dispersed over the alumina carrier. The presence of a highly dispersed La phase is consistent with conclusions drawn by Yang and Swartz[25] from XRD studies of catalysts with La loadings similar to those of our study. In addition, Alvero et al.[26] have used the absence of X-ray diffraction and Raman peaks of La_2O_3 to propose that La is highly dispersed on a 10% La_2O_3/Al_2O_3 catalyst.

Structure of Cobalt/Lanthanum/Alumina Catalysts. 1. Co/Al_2O_3 Catalyst. XRD and Raman analyses of the unpromoted Co/Al_2O_3 catalyst indicate that a significant fraction of the cobalt phase is present as Co_3O_4. Assuming that Co_3O_4 is the only reducible species, gravimetric data suggest that approximately 85% of the cobalt is present as Co_3O_4. The peak shape of the ESCA Co $2p_{3/2}$ spectrum measured for the unpromoted Co/Al_2O_3 catalyst is similar to that observed for $CoAl_2O_4$.[27] This apparent discrepancy between the cobalt species determined by ESCA and bulk measurements may be readily understood when one considers the structure of a Co/Al_2O_3 catalyst. It is well-known[28,29] that at least two phases exist on the surface of Co/Al_2O_3 catalysts: discrete Co_3O_4 particles and a surface spinel consisting of Co^{2+} ions in octahedral and tetrahedral sites of the alumina lattice. In principle, photoelectrons from the Co_3O_4 particles and the surface phase will contribute to the ESCA Co $2p_{3/2}$ spectrum. However, due to the high dispersion of the surface spinel relative to the Co_3O_4 phase, the qualitative features of the ESCA spectrum will be more representative of the surface spinel.

The ESCA Co/Al intensity ratio measured for the dried catalyst is slightly higher than the value predicted for monolayer dispersion. This suggests that the cobalt phase is well-dispersed in the dried catalyst. The pronounced decrease in Co/Al intensity ratio following calcination indicates that, during calcination, decomposition of the cobalt nitrate and aggregation of Co_3O_4 occur. These results agree with X-ray diffraction line broadening calculations that indicate the presence of large (~11.8 nm) Co_3O_4 particles in the unpromoted catalyst.

The discrepancy between the cobalt metal dispersion calculated for the unpromoted Co/Al_2O_3 catalyst by using H_2 chemisorption and ESCA data may be understood in terms of the limitations of the two techniques. Calculation of particle sizes using ESCA intensity ratios is affected by approximations in the Kerkhof–Moulijn model such as the cubic shape assumed for the supported particles and the sheet structure adopted for the carrier. Chemisorption results may also be affected by several variables. Reoxidation of the metal surface by hydroxyl groups may occur during the evacuation step of the chemisorption experiment. Furthermore, as noted by Matyi et al.,[30] particle sizes calculated from chemisorption data may be subject to significant error due to the geometry assumed for the supported particles. The density of surface sites present in cubes, spheres, and disks may be significantly different, resulting in different uptakes of probe gases on particles with the same surface area. We believe that the ESCA results more accurately reflect the true dispersion of the cobalt metal. This assertion is based on XRD studies of the reduced Co/Al_2O_3 catalyst which suggest the presence of ~10.0-nm (maximum) cobalt metal crystallites. This indicates a dispersion of approximately 10%, which is closer to the value determined from ESCA calculations (~11%) than that obtained from H_2 chemisorption results (~5%).

2. Co/La/Al_2O_3 Catalysts. Our study indicates that the influence of lanthanum on the structure of the CoLay catalyst depends on the La content. Two levels of lanthanum loading will be discussed: La/Al atomic ratios ≤0.026 (low loadings) and La/Al > 0.026 (high loadings).

For CoLay catalysts with low La loadings (La/Al ≤0.026), XRD and Raman data indicate that addition of lanthanum has little effect on the amount of Co_3O_4 on the catalysts. This is consistent with the limited effect that lanthanum addition has on the reducibility of the cobalt phase. The absence of any significant variation in the Co_3O_4 particle size determined from XRD line broadening calculations indicates that the dispersion of Co_3O_4 is not significantly affected by lanthanum addition. This is consistent with the similarity of the Co/Al intensity ratios measured for the calcined unpromoted catalyst and calcined CoLay catalysts with La/Al atomic ratios ≤0.026.

For catalysts with high La loadings (La/Al > 0.026), the decrease in intensity of the Co_3O_4 X-ray diffraction peaks with increasing La loading may be attributed either to an increae in the dispersion of Co_3O_4 or to a decrease in the amount of Co_3O_4. The parallel decrease in Co_3O_4 Raman peak intensities observed for catalysts with La/Al atomic ratios >0.026 indicates clearly that there is a decrease in the amount of Co_3O_4 on the catalysts. We ascribe this decrease in Co_3O_4 to formation of a La–Co mixed oxide. This is consistent with the decrease in cobalt reducibility observed for La-rich CoLay catalysts. Since lanthanum oxides are less reducible than Co_3O_4, the reducibility of the La–Co mixed oxide is likely to be lower than that measured for Co_3O_4.[30] The increase in ESCA Co/Al intensity ratio observed for La-rich catalysts indicates that the La–Co mixed oxide is well-dispersed relative to the Co_3O_4 phase.

For La-rich catalysts, the less pronounced decrease in ESCA Co/Al intensity ratios observed following calcination of the dried catalysts (relative to the decrease observed for catalysts with low

(25) Yang, J. Y.; Swartz, W. E. *Spectrosc. Lett.* **1984**, *17*(6, 7), 331–343.
(26) Alvero, R.; Bernal, A.; Carrizosa, I.; Odriozola, J. A. *Inorg. Chim. Acta* **1987**, *140*, 45–47.
(27) Chin, R. L.; Hercules, D. M. *J. Phys. Chem.* **1982**, *86*, 3079–3089.
(28) Ashley, J. H.; Mitchell, P. C. H. *J. Chem. Soc. A* **1969**, 2730–2735.
(29) Lo Jacono, M.; Cimino, A.; Schuit, G. C. A. *Gazz. Chim. Ital.* **1973**, *103*, 1281–1295.
(30) Matyi, R. J.; Schwartz, C. H.; Butt, J. B. *Catal. Rev.—Sci. Eng.* **1987**, *29*(1), 41–99.
(31) Boldyrev, V. V.; Bulens, M.; Delmon, B. *Stud. Surf. Sci. Catal.* **1979**, *2*.

La loadings) suggests that the high dispersion of the mixed oxide can be ascribed to less agglomeration of the cobalt phase (Figure 5). This can be attributed to interaction of the cobalt species with the La-rich alumina during cobalt impregnation and calcination. The increase in La/Al intensity ratio following impregnation indeed suggests that La phases dissolve in the impregnating solution containing the cobalt salt. The solvated La^{3+} and Co^{2+} ions will deposit onto the alumina support during the drying step. Interaction between La and Co deposited on the support decreases the agglomeration of the cobalt phase during calcination.

The discrepancy between the cobalt metal dispersion calculated from H_2 chemisorption and ESCA data for La-rich CoLay catalysts may be attributed in part to the activated nature of H_2 chemisorption over well-dispersed cobalt catalysts. Reuel and Bartholomew[32] have reported that the suppression of H_2 chemisorption increases with increasing cobalt dispersion. An alternate explanation for the suppression may involve blockage of cobalt metal sites by lanthanum oxide moieties on the surface of the metal particles. Barrault et al.[1] have given a similar explanation for suppression of chemisorption on CoLa catalyst supported on carbon. They proposed that surface sites are blocked by reduced LaO_x moieties that migrate to the surface of the metal particles during reduction. In our system, we believe that decoration of the cobalt phase by La is more likely to occur during cobalt impregnation. This is consistent with the observed increase in ESCA La/Al intensity ratio following cobalt impregnation.

Model for the Structure of CoLay Catalysts. Based on the discussion above, a tentative model for the structure of the CoLay catalyst can be proposed. Two levels of La loadings must be considered: La/Al $\leq$0.026 and La/Al >0.026. For Lay catalysts with low La loadings (La/Al $\leq$0.026), a well-dispersed La–Al_2O_3 interaction species exists on the surface of the Lay catalysts; however, only a relatively small amount of lanthanum is available to react with the cobalt during impregnation and calcination. Thus, CoLay catalysts with low La loadings have structures very similar to the unpromoted Co/Al_2O_3 catalyst. In this case, most of the cobalt is present as large particles of Co_3O_4. The remaining cobalt is present as a highly dispersed surface compound similar to $CoAl_2O_4$.[24] Following reduction, most cobalt is present as large particles of cobalt metal supported on the lanthanum-modified carrier.

For Lay catalysts with high La loadings (La/Al >0.026), the amount of lanthanum available to interact with cobalt during impregnation and calcination increases with increasing La content. Thus, increasing the La content of the Lay supports produces a CoLay catalyst with less Co_3O_4 and a highly dispersed La–Co mixed oxide. The Co_3O_4 phase formed on La-rich catalysts is better dispersed than the Co_3O_4 present in the unpromoted catalyst. Following reduction, part of the cobalt metal phase is present as crystallites formed by reduction of Co_3O_4. Highly dispersed metal particles are also present from reduction of La–Co mixed oxide phases. The unreduced fraction of cobalt is present as a highly dispersed surface phase.

The exact nature of the La–Co mixed oxide is unknown at this time. Both XRD and Raman studies of the CoLay catalysts detected no peaks other than those of Co_3O_4. One possible structure for the mixed oxide is well-dispersed $LaCoO_3$. Small particles of $LaCoO_3$ (<3.0 nm) would not be detected by XRD. We do not expect Raman spectra of the catalysts to show peaks for $LaCoO_3$ since no peaks were observed in the Raman spectrum of the $LaCoO_3$ standard compound. This is consistent with reports that perovskite structures are generally weak second-order Raman scatterers.[33] However, the ESCA Co $2p_{3/2}$ binding energies measured for the La-rich catalysts are 1.6 eV higher than the value measured for $LaCoO_3$. In addition, we must note that preliminary EXAFS data are not consistent with $LaCoO_3$ formation.[34] Thus, we tentatively describe the mixed oxide as a highly dispersed La–Co mixed oxide that interacts strongly with the support.

Structure of Lanthanum/Cobalt/Alumina Catalysts. The results of this study indicate that addition of lanthanum after cobalt has little effect on the structure of the LayCo catalysts. This is illustrated by the absence of any significant variation in Co_3O_4 Raman and XRD intensities or cobalt reducibility as a function of La content. ESCA results for the Co $2p_{3/2}$ binding energy and Co/Al intensity ratios also indicate that the surface structure of the LayCo catalysts is not significantly affected by the addition of lanthanum.

The lack of any significant change in the structure of the LayCo catalysts as a function of lanthanum content may be understood in terms of the structure of the unmodified Co/Al_2O_3 catalyst. A large fraction (~85%) of the cobalt phase present in the unpromoted Co/Al_2O_3 catalyst is poorly dispersed crystalline Co_3O_4 (~12.5 nm). Thus, approximately 95% of the alumina surface is exposed to impregnating solution. During impregnation of the Co/Al_2O_3 catalyst with solutions of $La(NO_3)_3$, the La species interacts with the alumina and the surface of large Co_3O_4 particles. Thus, we expect the lanthanum to affect only a small fraction of the Co_3O_4 particles.

Influence of La on the CO Hydrogenation Activity and Selectivity of Cobalt/Alumina Catalysts. For CoLay catalysts with low La loadings (La/Al $\leq$0.043), addition of lanthanum has little effect on the turnover frequency for CO hydrogenation (Figure 6). This is consistent with structural information described earlier which showed that, for such catalysts, addition of La had little effect on the chemical state and dispersion of the cobalt phase.

The decrease in TOF observed for high La loadings parallels the decrease in Co_3O_4 intensities measured by XRD and Raman spectroscopy (Figure 3). One explanation for this similarity could be that the active phase for CO hydrogenation is obtained primarily from reduction of Co_3O_4 crystallites. This assumes that the highly dispersed cobalt metal derived from the La–Co mixed oxide is not active in CO hydrogenation. This is consistent with the low TOF for CO hydrogenation reported for catalysts containing small Co metal particles.[35,36] Assuming that cobalt metal derived from Co_3O_4 is the only active phase for CO hydrogenation, the catalytic activity can be predicted on the basis of the amount of Co_3O_4 and the dispersion of Co metal. The amount of Co_3O_4 can be calculated from Raman data by assuming that the change in Co_3O_4 intensity is linearly related to the change in Co_3O_4 concentration. Thus, we can estimate the CO hydrogenation rate for the series of CoLay catalysts by multiplying the rate measured for the CoLa0 catalyst by the relative amount of Co_3O_4 in each catalyst. It should be noted that the rates calculated in this manner are not corrected for differences in the dispersion of the cobalt phase. The estimate of Co metal dispersion derived from reduction of Co_3O_4 is not straightforward. In principle, H_2 chemisorbs on all available Co metal sites. However, it is well-known that H_2 chemisorption is suppressed on small particles of cobalt.[32] Thus, if we assume that H_2 chemisorption data reflect only dispersion of cobalt metal crystallites derived from reduction of large Co_3O_4 particles, then rates predicted from Raman data can be corrected for particle size. Variation of the rate per gram of cobalt measured (closed circles) and predicted values corrected for dispersion (open circles) is given for the CoLay catalysts as a function of La/Al atomic ratio in Figure 8. One can see that predicted rates corrected for cobalt dispersion (open squares) agree very well with the measured values.

Barrault et al.[1] have reported that a lanthanum-promoted cobalt catalyst supported on carbon has a higher TOF for CO hydrogenation than the unpromoted Co/carbon catalyst. These authors attributed promotion to the formation of new active sites by migration of partially reduced LaO_x moieties to the surface of the metal particles during pretreatment. However, the particle size of the cobalt metal crystallites was difficult to determine presumably because of the coverage of the cobalt metal sites by reduced LaO_x moieties. Since the TOF for CO hydrogenation

(32) Reuel, R. C.; Bartholomew, C. H. *J. Catal.* **1984**, *85*, 63–77.
(33) *Inorganic Infrared and Raman Spectra*; Ross, S. D., Ed.; McGraw-Hill: London, 1972; p 108.
(34) Hoffmann, D. P.; Proctor, A.; Fay, M.; Ledford, J. S.; Hercules, D. M. Manuscript in preparation.
(35) Fu, L.; Bartholomew, C. H. *J. Catal.* **1985**, *92*, 376–387.
(36) Reuel, R. C.; Bartholomew, C. H. *J. Catal.* **1984**, *85*, 78–88.

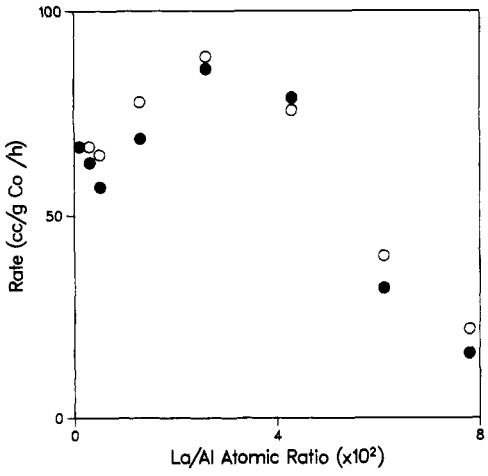

Figure 8. Variation of the rate for CO hydrogenation measured (●) and predicted values corrected by dispersion estimated from H_2 chemisorption (○) for the CoLay catalysts as a function of La/Al atomic ratio.

over cobalt catalysts depends on the dispersion of the active phase, part of the promotion effect ascribed to lanthanum may be due to a decrease in cobalt dispersion reported for the La-promoted catalyst.

Addition of lanthanum to the CoLay catalysts increases the selectivity to higher hydrocarbons and olefins (Table III). The most pronounced increase in selectivity occurs for catalysts with La/Al atomic ratios >0.013. We attribute this increased selectivity to the formation of lanthanum-promoted sites on the catalyst. These sites may involve lanthanum moieties on the surface of large cobalt metal particles. As noted earlier, we believe that decoration of the cobalt phase by La can occur during cobalt impregnation. This is consistent with higher La/Al intensity ratios observed for CoLay catalysts relative to Lay carriers. The ability of basic promoters to increase the selectivity to higher hydrocarbons and olefins is a well-known feature of Fischer–Tropsch catalysts.[37-41] Barrault et al.[1] have also reported that La promotion of a carbon-supported cobalt catalyst increases the selectivity to higher hydrocarbons and olefins. They attributed the increased selectivity to changes in the electronic state and dispersion of the cobalt metal as well as the creation of new reaction sites. Similar increases in selectivity to higher hydrocarbons and olefins have been reported for Ru catalysts supported on La_2O_3 instead of SiO_2.[10] In this case, the authors attribute changes in olefin selectivity to an increase in the rate of olefin desorption relative to the rate of olefin hydrogenation.

In our work, catalysts prepared by reverse impregnation (LayCo) were examined to separate the effects of La addition and cobalt dispersion on the catalytic properties of a Co/Al_2O_3 catalyst. The results show that addition of lanthanum after cobalt does not affect the TOF for CO hydrogenation or the selectivity to higher hydrocarbons and olefins. These results suggest that, during lanthanum impregnation and subsequent calcination, the lanthanum phase preferentially interacts with the Al_2O_3 support. Preliminary study of the La impregnation process suggests however that the selectivity to higher hydrocarbons and olefins can be enhanced by the use of solutions in excess of the pore volume of the Co/Al_2O_3 catalyst.[42]

Conclusions

The combined use of several techniques to investigate the effect of La addition on the structure and CO hydrogenation activity of Co/Al_2O_3 catalysts leads to the following conclusions.

1. ESCA data indicate that lanthanum is highly dispersed over the alumina carrier.

2. The unpromoted Co/Al_2O_3 catalyst contains primarily large particles of Co_3O_4 and a dispersed surface compound similar to $CoAl_2O_4$, in agreement with previously reported results.[24] For CoLay catalysts with low La contents (up to La/Al = 0.013), the presence of lanthanum has little influence on the supported cobalt oxide or the activity and selectivity of the reduced catalyst in CO hydrogenation.

3. For CoLay catalysts with higher La loadings (La/Al > 0.026), the Co_3O_4 cobalt phase is suppressed in favor of a dispersed amorphous La–Co mixed oxide. ESCA and H_2 chemisorption data indicate enhanced dispersion of the metallic cobalt phase with increasing La content. The TOF for CO hydrogenation decreases dramatically for high La loadings. This has been attributed to a decrease in the amount of Co_3O_4 in the catalysts.

4. Catalysts prepared by reverse impregnation (LayCo) show little evidence of Co–La interaction. No significant variation in reducibility or cobalt metal dispersion is observed. The addition of La has little effect on the TOF for CO hydrogenation or selectivity to higher hydrocarbons and olefins.

Acknowledgment. This work was supported by the National Science Foundation under Grants CHE-8411835 and CHE-8401202. J. S. Ledford acknowledges the A. W. Mellon Educational and Charitable Trust for a Predoctoral Fellowship.

Registry No. Co, 7440-48-4; La, 7439-91-0; H_2, 1333-74-0.

(37) Anderson, R. B. In *Catalysis*; Emmett, P. H., Ed.; Reinhold: New York, 1956; Vol. IV, p 123.
(38) Anderson, R. B.; Karn, F. S.; Schultz, J. F. *J. Catal.* **1965**, *4*, 56–65.
(39) Dory, M. E.; Shingles, T.; Boshoff, L. J.; Oosthuizen, G. J. *J. Catal.* **1969**, *15*, 190–199.
(40) Martin, G. A. *Stud. Surf. Sci. Catal.* **1982**, *11*, 315–335.
(41) Snel, R. *Catal. Rev.—Sci. Eng.* **1987**, *29*(4), 361–445.
(42) Ledford, J. S.; Houalla, M.; Hercules, D. M. Manuscript in preparation.